J. Fluid Mech. (1995), *vol.* 297, *pp.* 293–305

Flow focusing instability in a solidifying mushy layer

By A. O. P. CHIARELI AND M. GRAE WORSTER

Institute of Theoretical Geophysics, Department of Applied Mathematics and Theoretical Physics, University of Cambridge, Silver Street, Cambridge CB3 9EW, UK

(Received 16 December 1994)

The stability of the flow of interstitial liquid in a mushy layer driven by expansion or contraction upon solidification is analysed. The full perturbation equations are reduced in a particular aymptotic limit that allows the principal mechanisms controlling instability to be identified. Comparisons are made with the acid-etching instabilities in porous rocks. The full equations are then solved to determine the parametric dependences of the instability. It is found that, though the potential for instability exists, it is unlikely to occur in practice.

1. Introduction

When fluid flows through a porous medium and reacts with the medium to alter its permeability, an instability can result whereby the flow becomes focused into narrow fingers or channels. A previously studied example of this occurs during enhanced oil recovery, when acid is pumped through oil-bearing porous rocks in order to increase the permeability of the rock and stimulate the extraction of oil. It has been determined (Chadam *et al.* 1986; Sherwood 1987; Hinch & Bhatt 1990) that a propagating planar reaction front or reaction zone, in which the acid partially dissolves the rock, suffers an instability that results in the front being distorted into fingers and the preferential flow of acid along these fingers.

Another example of such focusing is sometimes observed during the solidification of alloys when a mushy layer forms. A mushy layer is a porous medium comprising a matrix of crystals bathed in the melt from which they grew. Convection driven by compositional buoyancy is observed in some cases to produce within the mushy layer vertical channels (chimneys) of zero solid fraction from which emanate plumes of relatively dilute fluid (Copley *et al.* 1970). In this case, the primary linear instability is due to buoyancy forces (Fowler 1985; Worster 1992*a*; Emms & Fowler 1994; Chen, Lu & Yang 1994). Focusing of the convection into narrow regions of upflow results nonlinearly from local increases in permeability as crystals are redissolved within the mushy layer (Tait, Jahrling & Jaupart 1992; Amberg & Homsy 1993). Such dissolution can occur in mushy layers when there is a component of the flow of the interstitial liquid in the direction of the temperature gradient (Flemings 1974; Fowler 1985).

Chimneys formed in mushy layers during casting produce structural and compositional inhomogeneities that can be detrimental to the product being manufactured. For this reason, it has been proposed that casting of high-perfomance alloys might benefit from being done in Space, where the micro-gravitational environment will weaken or eliminate buoyancy-driven convection within the mushy layer. However,

in any environment, interstitial flow can be driven purely by the expansion (or contraction) of the alloy during solidification. In this paper, we investigate the stability of such flows to determine whether inhomogeneities in a casting might be caused by this mechanism in the absence of buoyancy-driven convection. This study provides new insight into the interactions between solidification and flow within mushy layers via a relatively straightforward linear analysis and, more generally, extends our understanding of flow through reactive porous media.

The equations governing solidification of a mushy layer at constant speed in the absence of buoyancy forces are presented in §2 and a steady analytic solution of these equations is derived in §3. This solution provides the basic state for a linear stability analysis, which is described in full generality in §4. The equations describing the mushy layer are very complex with many independent dimensionless parameters. A special limit is taken in §5 that reduces the system of equations to the bare essentials required to describe the physical interactions that can lead to instability. The reduced system is solved to determine the character of the dispersion relation, which is compared and contrasted with previous results for reacting flows in porous media. In §6, the full perturbation equations are solved numerically to determine how the conditions for instability vary with the dimensionless parameters of the solidifying system. The implications of this study are discussed in the concluding section.

2. Governing equations

The geometry of the system to be analysed is illustrated in figure 1. An alloy is being cast directionally at constant speed V. The domain of primary interest to us is the mushy layer that separates the completely solid region, which exists at temperatures below the eutectic point, from the completely liquid melt. In a Cartesian frame of reference (x, y, z) moving with speed V in the z-direction, the eutectic front is assumed to remain fixed at $z = 0$ while the mush–liquid interface $z = h(x, y, t)$ is a free boundary to be determined as part of the solution. The temperature is equal to the eutectic temperature T_e at $z = 0$ and increases with z to T_∞ far from the region of solidification, where the concentration of the melt is C_0. The solid and liquid are taken to have different, uniform and constant densities ρ_s and ρ_l. The compositional diffusivity is assumed to be zero in the solid phase, while all other physical and thermal properties are assumed to be the same in each phase.

Dimensionless variables are introduced by scaling the fluid velocity $\boldsymbol{U}$ with the solidification rate V, distances with the thermal-diffusion lengthscale $l_\kappa = \kappa/V$, time t with κ/V^2 and pressure p with $\mu V/\Pi^*$, where κ is the thermal diffusivity, μ is the dynamic viscosity of the liquid, and Π^* is a characteristic permeability of the mushy layer. Dimensionless variables for temperature and concentration are defined by

$$\theta = \frac{T - T_L(C_0)}{\Delta T} \quad \text{and} \quad \Theta = -\frac{C - C_0}{\Delta C}, \tag{2.1a,b}$$

where $\Delta T = \Gamma \Delta C = T_L(C_0) - T_e$, and $T_L(C)$ is the liquidus relationship, which is assumed to be linear with slope $-\Gamma$.

The governing equations in the fully liquid region, $z > h$, are diffusion-advection equations for heat and solute and the Navier–Stokes equations

$$\frac{\partial \theta}{\partial t} - \frac{\partial \theta}{\partial z} + \boldsymbol{U} \cdot \nabla \theta = \nabla^2 \theta, \tag{2.2}$$

$$\frac{\partial \Theta}{\partial t} - \frac{\partial \Theta}{\partial z} + \boldsymbol{U} \cdot \nabla \Theta = \epsilon \nabla^2 \Theta, \tag{2.3}$$

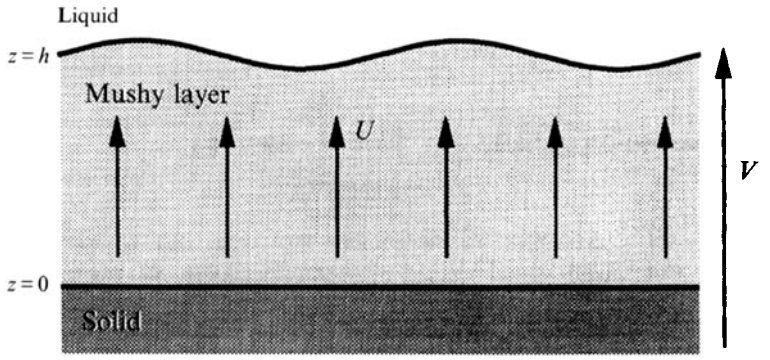

FIGURE 1. A schematic diagram of the proposed problem. A mushy layer is growing at a constant speed V in the absence of gravity. There is a flow in the interior of the mushy layer created by expansion as the melt solidifies. The eutectic front $z = 0$ is assumed to remain planar, while the mush–liquid interface $z = h(x, t)$ is free to deform.

$$\frac{1}{\sigma}\left(\frac{\partial \boldsymbol{U}}{\partial t} - \frac{\partial \boldsymbol{U}}{\partial z} + \boldsymbol{U}\cdot\nabla\boldsymbol{U}\right) = \nabla^2\boldsymbol{U} - \mathscr{H}\nabla p, \tag{2.4}$$

$$\nabla\cdot\boldsymbol{U} = 0, \tag{2.5}$$

where $\epsilon = D/\kappa$ is the ratio of diffusivities of solute and heat, $\sigma = \nu/\kappa$ is the Prandtl number, and $\mathscr{H} = l_\kappa^2/\Pi^*$ is a mobility ratio. The parameter $\mathscr{H}$, which is typically very large, can be thought of as the square of the ratio of the thermal lengthscale (on which the depth of the mushy layer principally depends) to the average spacing between dendrites within the mushy layer.

The boundary conditions for the liquid region are

$$\Theta \to 0, \quad \theta \to \theta_\infty, \quad \boldsymbol{U} \to (1-r)\hat{\boldsymbol{z}} \qquad (z \to \infty), \tag{2.6a–c}$$

$$\theta = \Theta, \quad \boldsymbol{n}\cdot\nabla\theta = \boldsymbol{n}\cdot\nabla\Theta, \quad [\boldsymbol{n}\cdot\boldsymbol{U}] = 0, \quad \boldsymbol{U} - (\boldsymbol{n}\cdot\boldsymbol{U})\boldsymbol{n} = 0 \qquad (z = h), \tag{2.7a–d}$$

where $r = \rho_s/\rho_l$, $\theta_\infty = (T_\infty - T_L(C_0))/\Delta T$ is the dimensionless far-field temperature, $\boldsymbol{n}$ is the unit normal to the mush–liquid interface, pointing into the liquid, and where [ ] denotes a jump in the enclosed quantity across the interface. The far-field boundary condition on the velocity field (2.6*c*) is determined by global mass conservation. Condition (2.7*a*) is the liquidus relationship applied at the interface, while (2.7*b*) is the condition of marginal equilibrium (Worster 1986). Conditions (2.7*c*) and (2.7*d*) express continuity of the normal mass flux across the mush–liquid interface and the no-slip condition applied to the liquid adjacent to the interface with the mushy layer, respectively.

Local thermodynamic equilibrium prevails throughout the mushy layer, so that $\theta \equiv \Theta$ in $0 < z < h$. The governing equations there are

$$\frac{\partial\theta}{\partial t} - \frac{\partial\theta}{\partial z} + \boldsymbol{U}\cdot\nabla\theta = \nabla^2\theta + \mathscr{S}\left(\frac{\partial\phi}{\partial t} - \frac{\partial\phi}{\partial z}\right), \tag{2.8}$$

representing conservation of heat,

$$(1-\phi)\left(\frac{\partial\theta}{\partial t} - \frac{\partial\theta}{\partial z}\right) + \boldsymbol{U}\cdot\nabla\theta = r(\theta - \mathscr{C})\left(\frac{\partial\phi}{\partial t} - \frac{\partial\phi}{\partial z}\right), \tag{2.9}$$

representing conservation of solute,

$$\nabla \cdot \boldsymbol{U} = (1-r)\left(\frac{\partial \phi}{\partial t} - \frac{\partial \phi}{\partial z}\right), \tag{2.10}$$

representing conservation of mass, and Darcy's equation

$$\boldsymbol{U} = -\Pi(\chi)\nabla p. \tag{2.11}$$

The permeability Π is assumed to be locally isotropic but to vary with the local porosity $\chi = 1 - \phi$. Note that, within the mushy layer, $\boldsymbol{U}$ represents the Darcy velocity, i.e. the mean volume flux per unit area. These equations, in which the effects of expansion are incorporated, have been presented previously and their derivation discussed by Worster (1992*b*) and by Chiareli, Huppert & Worster (1994).

The dimensionless parameters governing this system of equations are r, θ_∞, the Stefan number

$$\mathscr{S} = \frac{\rho_s L}{\rho_l C_p \Delta T}, \tag{2.12}$$

where L is the latent heat of fusion per unit mass and C_p is the specific heat capacity, and a concentration ratio

$$\mathscr{C} = \frac{C_0 - C_s}{\Delta C}, \tag{2.13}$$

where C_s is the composition of the solid phase within the mushy layer.

The key feature of the present study, which has the potential of causing flow-focusing instabilities, is that the permeability $\Pi(\chi)$ is a function of the local liquid fraction χ. Many empirical formulae have been determined for the permeabilities of various porous media (Bear 1988). Here, we investigate the simple family of functions

$$\Pi(\chi) = \chi^{\mathscr{P}}, \tag{2.14}$$

where $\mathscr{P}$ is a constant that represents the sensitivity of the permeability to changes in porosity. The sensitivity can be defined as

$$\frac{1}{\Pi}\frac{\mathrm{d}\Pi}{\mathrm{d}\chi} = \frac{\mathscr{P}}{\chi} \tag{2.15}$$

which is directly proportional to $\mathscr{P}$ and in general is a function of position in the mushy layer owing to the variation of porosity χ.

The boundary conditions for the mushy layer are

$$\theta = -1, \quad W = (1-r)(1-\phi) \qquad (z = 0) \tag{2.16a,b}$$

and

$$[\theta] = 0, \quad \phi = 0, \quad [\boldsymbol{n}\cdot\nabla\theta] = 0, \quad [p] = 0 \qquad (z = h), \tag{2.17a–d}$$

where W is the z-component of velocity. Condition (2.16*b*) is a consequence of mass conservation at the eutectic front, while conditions (2.17*b*) and (2.17*c*) are derived from the expressions for conservation of heat and solute once the condition of marginal equilibrium is taken into account.

3. A steady solution

The equations presented in the previous section admit a steady, one-dimensional solution that depends only on z. This is an extension of the steady solution that has been found previously for the case of no expansion or contraction (Hills, Loper &

Roberts 1983; Worster 1991). In one dimension, the velocity field $\boldsymbol{U} = W_0\hat{\boldsymbol{z}}$ can be determined from the mass conservation equation (2.10) to be

$$W_0 = (1 - r) \tag{3.1}$$

in the liquid region and

$$W_0 = (1 - r)(1 - \phi_0) \tag{3.2}$$

in the mushy region. Equations (2.2) and (2.3) are then readily integrated to give

$$\theta_0 = \theta_\infty + (\theta_i - \theta_\infty)\mathrm{e}^{-r(z-h_0)} \tag{3.3}$$

and

$$\Theta_0 = \theta_i \mathrm{e}^{-r(z-h_0)/\epsilon}, \tag{3.4}$$

once the boundary conditions (2.6) and (2.7*a*) are taken into account. The temperature at the mush–liquid interface θ_i is determined from (2.7*b*) to be

$$\theta_i = -\frac{\epsilon}{1-\epsilon}\theta_\infty. \tag{3.5}$$

We shall adopt the limit $\epsilon \to 0$, which is physically reasonable since typically $D \ll \kappa$, so the dimensionless interfacial temperature/concentration becomes

$$\theta_i = 0, \tag{3.6}$$

which then also gives $\Theta \equiv 0$ in the liquid region.

In the mushy layer, the solid fraction ϕ_0 is determined by integrating the equation of solute conservation (2.9) to obtain

$$\phi_0 = -\frac{\theta_0}{\mathscr{C} - \theta_0}, \tag{3.7}$$

using the boundary condition (2.17*b*). The equation of heat conservation (2.8) can be integrated once to give

$$\frac{\mathrm{d}\theta_0}{\mathrm{d}z} = r\theta_\infty - \theta_0 - \frac{\mathscr{S}\theta_0}{\mathscr{C} - \theta_0} - (1 - r)\mathscr{C}\ln\left(\frac{\mathscr{C} - \theta_0}{\mathscr{C}}\right). \tag{3.8}$$

The unperturbed depth of the mushy layer h_0 can be determined by inverting (3.8) to obtain $\mathrm{d}z/\mathrm{d}\theta_0$ and integrating from $\theta_0 = -1$ to $\theta_0 = 0$. Finally the pressure field is constant (zero) in the liquid region and, in the mushy region, is determined from Darcy's equation, which can be written as

$$\frac{\mathrm{d}p_0}{\mathrm{d}z} = -(1 - r)\frac{\chi_0}{\Pi(\chi_0)}. \tag{3.9}$$

We shall investigate these equations analytically in a special limit in §5 and numerically in §6, simultaneously with the perturbation equations derived in the next section.

4. Linear perturbation equations

The stability of the system is examined by determining the growth or decay of infinitesimal disturbances to the steady solution. The disturbed fields are written in the form

$$\begin{bmatrix} \theta \\ \boldsymbol{U} \\ p \\ \phi \end{bmatrix} = \begin{bmatrix} \theta_0(z) \\ (0, W_0(z)) \\ p_0(z) \\ \phi_0(z) \end{bmatrix} + \begin{bmatrix} \tilde{\theta}(z) \\ (\tilde{U}(z), \tilde{W}(z)) \\ \tilde{p}(z) \\ \tilde{\phi}(z) \end{bmatrix} \exp(\omega t + \mathrm{i}\alpha x), \tag{4.1}$$

where ω is the complex growth rate and α is the wavenumber parallel to the undisturbed interface. The concentration Θ remains identically zero in the liquid region. The governing equations are linearized about the basic state, which gives rise to the following perturbation equations and boundary conditions, in which we have dropped the tildes from the disturbance amplitudes and used primes to denote derivatives of the basic state.

In the liquid region,

$$\left[\mathrm{D}^2 + (\mathrm{D} - \omega) - W_0\mathrm{D} - \alpha^2\right]\theta = \theta_0' W, \tag{4.2}$$

$$(\mathrm{D}^2 - \alpha^2)W = \Omega, \tag{4.3}$$

$$\left[\mathrm{D}^2 - \frac{1}{\sigma}\{(W_0 - 1)\mathrm{D} + W_0' + \omega\} - \alpha^2\right]\Omega = 0, \tag{4.4}$$

where $\mathrm{D} \equiv \mathrm{d}/\mathrm{d}z$, and Ω is a variable representing the vertical component of the curl of vorticity which is introduced for convenience.

In the mushy region,

$$\left[\mathrm{D}^2 + (\mathrm{D} - \omega) - W_0\mathrm{D} - \alpha^2\right]\theta = \theta_0' W + \mathscr{S}(\mathrm{D} - \omega)\phi, \tag{4.5}$$

$$\left[(1 - \phi_0)\omega - (1 - \phi_0 - W_0)\mathrm{D} + r\phi_0'\right]\theta + \theta_0' W = \left[r(\mathscr{C} - \theta_0)(\mathrm{D} - \omega) - \theta_0'\right]\phi, \tag{4.6}$$

$$-(1 - r)(\mathrm{D} - \omega)\phi - \alpha^2 \Pi(\chi_0)p = \mathrm{D}W, \tag{4.7}$$

$$(1 - r)\mathscr{P}\phi + W = -\Pi(\chi_0)\mathrm{D}p. \tag{4.8}$$

These equations are subject to the linearized boundary conditions

$$\theta \to 0, \quad W \to 0, \quad \mathrm{D}W \to 0 \qquad (z \to \infty), \tag{4.9a–c}$$

$$\theta = -r\theta_\infty \eta, \quad [W] = (1 - r)\frac{r\theta_\infty}{\mathscr{C}}\eta, \quad \mathrm{D}W = 0 \quad (z = h_0+), \tag{4.10a–c}$$

$$[\theta] = 0, \quad [\mathrm{D}\theta] = -\mathscr{S}\frac{r\theta_\infty}{\mathscr{C}}\eta, \quad \phi = \frac{r\theta_\infty}{\mathscr{C}}\eta, \quad [p] = -[p_0']\eta \qquad (z = h_0-), \tag{4.11a–d}$$

$$\theta = 0, \quad W = -(1 - r)\phi \qquad (z = 0), \tag{4.12a, b}$$

where η is the perturbation to the position of the mush–liquid interface, i.e. $h(x, z, t) = h_0 + \eta(x, z, t)$. The interfacial condition on the pressure field (4.11*d*) can be used to determine

$$\mathrm{D}W_{\mathrm{mush}} = -\alpha^2(1 - r)\eta - (1 - r)(\mathrm{D} - \omega)\phi + \mathscr{H}^{-1}\left[\mathrm{D}\Omega + \frac{1}{\sigma}\{r(\Omega + \alpha^2 W) - \omega\mathrm{D}W\}\right]_{\mathrm{liquid}} \qquad (z = h_0), \tag{4.13}$$

which we approximate here by

$$\mathrm{D}W_{\mathrm{mush}} = -(1 - r)\left[\alpha^2\eta + (\mathrm{D} - \omega)\phi\right] \qquad (z = h_0) \tag{4.14}$$

on the assumption that $\mathscr{H} \gg 1$. Equivalently

$$p_{\mathrm{mush}} = (1 - r)\eta \qquad (z = h_0). \tag{4.15}$$

Note that this reduces to the condition of constant pressure used by Emms & Fowler (1994) in the case $r = 1$.

The perturbation equations presented in this section are quite complicated and will be solved numerically in §6. First, a reduced system will be derived and solved in §5, which will identify the fundamental mechanisms that control the instability of the flow in the mushy layer.

5. A reduced system

The equations governing the evolution of a mushy layer take a particularly simple form that nevertheless retains many of the significant physical interactions in what Fowler (1985) calls a 'near-eutectic' limit. In this limit, the solid fraction is small and the permeability is almost uniform. The important physical effects of permeability variations are retained by assuming that the sensitivity of the medium is large. Other simplifying features of this limit are that the basic-state temperature field is linear and the basic-state velocity field is uniform. In the present formulation, this limit is achieved by letting

$$\mathscr{C} \to \infty, \quad \theta_\infty \to \infty, \quad \text{with} \quad \frac{\mathscr{C}}{\theta_\infty} = O(1). \tag{5.1}$$

It is readily shown from the full equations given in §3 that, in this limit, the steady state of the mushy layer is given to leading order by

$$\boldsymbol{U}_0 = (0, 1-r), \quad \theta_0 = -1 + r\theta_\infty z, \quad \phi_0 = \mathscr{C}^{-1}(1 - r\theta_\infty z), \quad h_0 = \frac{1}{r\theta_\infty}. \tag{5.2a–d}$$

These solutions prompt the following rescaling of the variables and parameters:

$$\hat{\phi} = \mathscr{C}\phi, \quad \zeta = r\theta_\infty z, \quad \hat{\eta} = r\theta_\infty \eta, \quad \hat{\alpha} = \frac{\alpha}{r\theta_\infty}, \quad \hat{\omega} = \frac{\omega}{r\theta_\infty}. \tag{5.3a–e}$$

The leading-order perturbation equations in the mushy layer become

$$(\mathrm{D}_\zeta^2 - \hat{\alpha}^2)\theta = 0, \tag{5.4}$$

$$(\hat{\omega} - r\mathrm{D}_\zeta)\theta + W = r(\mathrm{D}_\zeta - \hat{\omega})\hat{\phi}, \tag{5.5}$$

$$(\mathrm{D}_\zeta^2 - \hat{\mathscr{P}}\mathrm{D}_\zeta - \hat{\alpha}^2)W = \hat{\alpha}^2(1-r)\hat{\mathscr{P}}\hat{\phi}, \tag{5.6}$$

where $\hat{\mathscr{P}} = \mathscr{P}/\mathscr{C}$. This scaling of $\mathscr{P}$ is necessary to retain the important effect of permeability variations in equation (5.6) once $\phi = \mathrm{O}(\mathscr{C}^{-1})$. For simplicity, we make the additional assumption that the position of the mush–liquid interface remains unperturbed (i.e. $\hat{\eta} = 0$), which could be achieved in principle by maintaining the temperature of the interface fixed. This is an *ad hoc* assumption that is not derived from the asymptotic scaling. Its effect is to decouple the mushy layer from the overlying liquid region, and it should not significantly affect the dynamics of the interior of the mushy layer. Therefore this reduced model will still give a good indication of the controlling mechanisms for dissolution that lead to focusing of the flow. The boundary conditions for the mushy layer are then

$$\theta = 0, \qquad W = 0 \qquad (\zeta = 0), \tag{5.7a, b}$$

$$\theta = 0, \qquad \mathrm{D}_\zeta W = 0, \qquad \hat{\phi} = 0 \qquad (\zeta = 1). \tag{5.8a–c}$$

Since the temperature perturbation satisfies a homogeneous equation (5.4) and boundary conditions (5.7*a*) and (5.8*a*), we deduce that $\theta \equiv 0$. The remaining third-order eigenvalue problem has solution

$$W = \sum_{n=1}^{3} a_n \mathrm{e}^{m_n(1-\zeta)}, \tag{5.9}$$

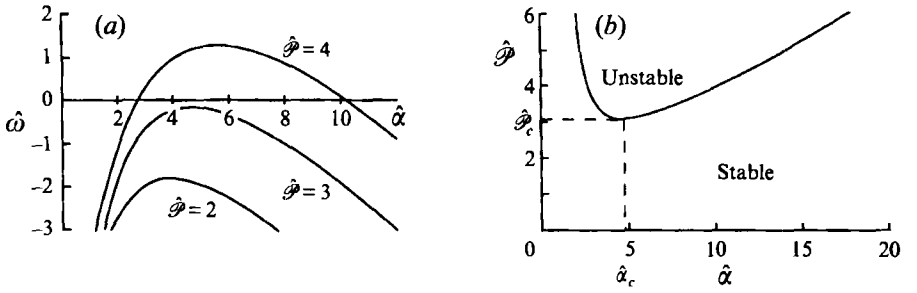

FIGURE 2. (*a*) Dispersion relation $\hat{\omega}$ *vs.* $\hat{\alpha}$ for equations in the 'near-eutectic' limit. It can be seen that the system is completely stable for small values of $\hat{\mathscr{P}}$, whereas, for sufficiently large values of $\hat{\mathscr{P}}$, there is a range of unstable wavenumbers $\hat{\alpha}$ bounded away from zero and infinity. (*b*) A marginal stability curve $\hat{\mathscr{P}}$ *vs.* $\hat{\alpha}$ showing the critical value $\hat{\mathscr{P}}_c$, which is defined as the minimum value of the permeability variation parameter for which the system is unstable. These curves were calculated with $r = 0.5$.

where m_n are the roots of

$$(m^2 + \mathscr{P}m - \hat{\alpha}^2)(m + \hat{\omega}) + \hat{\alpha}^2 \left(\frac{1-r}{r}\right)\hat{\mathscr{P}} = 0. \tag{5.10}$$

The boundary conditions (5.7) and (5.8) give the eigenvalue equation

$$\begin{vmatrix} e^{m_1} & e^{m_2} & e^{m_3} \\ m_1 & m_2 & m_3 \\ m_1^2 - \alpha^2 & m_2^2 - \alpha^2 & m_3^2 - \alpha^2 \end{vmatrix} = 0, \tag{5.11}$$

which is an algebraic equation for $\hat{\omega}(\hat{\mathscr{P}}, \hat{\alpha})$. The calculations of $\hat{\omega}$ were done partly symbolically and partly numerically using Mathematica. Illustrative results are shown in figure 2. It can be seen that the system is completely stable for small values of $\hat{\mathscr{P}}$, whereas, for sufficiently large values of $\hat{\mathscr{P}}$, there is a range of unstable wavenumbers bounded away from zero and infinity.

It is interesting to contrast this behaviour with the results of stability analyses of forced flow through reactive porous media (figure 3). Sherwood (1987) considered a reaction front of zero thickness and found that the growth rate ω increased logarithmically with wavenumber α as $\alpha \to \infty$. Hinch & Bhatt (1990) considered a reaction front of finite thickness and found, by contrast, that ω tended to a constant as $\alpha \to \infty$. Neither of these studies included the effects of diffusion of reactant. Chadam *et al.* (1986) did include such diffusion and found that short-wavelength disturbances were thus stabilized. All three of these studies found the same behaviour at small wavenumbers; namely that disturbances of zero wavenumber are neutrally stable, while disturbances of small but finite wavenumber (long wavelength) are unstable. These studies thus all concluded that a reacting flow through a porous medium is unconditionally unstable. In our study, the reacting porous medium is the mushy layer.

There are two critical differences between these previous studies and the present. One is that here the porous medium is finite in extent, rather than infinite, which suppresses long-wavelength perturbations to the pressure field. The other difference is that overall the mushy layer is solidifying, which means that small perturbations can 'heal' if they are advected (by the moving frame) through their own length faster than the local rate of dissolution caused by the flow.

This is quite a different mechanism for the stabilization of short-wavelength disturbances than the diffusive mechanism incorporated in the study by Chadam *et al.*

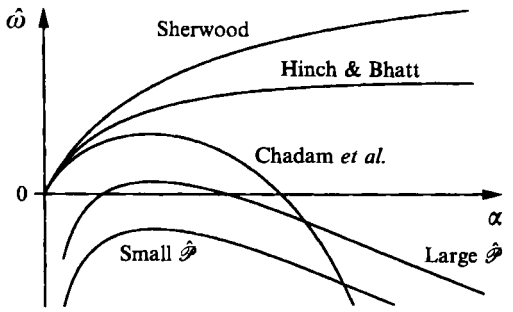

FIGURE 3. A comparison between the dispersion relation obtained in this paper and those obtained in various studies of forced flow through reactive porous media (Sherwood 1987; Hinch & Bhatt 1990; Chadam *et al.* 1986).

(1986). It is characterized by the decay rate being proportional to α, when α is large, rather than α^2, the latter being characteristic of diffusive damping. Note that diffusion is restored as the chief damping mechanism in the full perturbation equations analysed in the next section.

6. Critical conditions for instability

The fully liquid region is expected to have little influence on the instability being analysed here. Its hydrodynamic influence is negligible in the limit $\mathscr{H} \gg 1$, as discussed in the previous section, while its thermodynamic influence is felt only through the Stefan condition (4.11*b*). We proceed on the assumption that the perturbation to the heat flux from the liquid is negligible and solve (4.5)–(4.8) using boundary conditions

$$\theta = -r\theta_\infty \eta, \quad D\theta = \frac{r\mathscr{S}\theta_\infty}{\mathscr{C}}\eta, \quad \phi = \frac{r\theta_\infty}{\mathscr{C}}\eta, \quad [p] = (1-r)\eta \qquad (z = h_0), \qquad (6.1a\text{–}d)$$

$$\theta = 0, \quad W = -(1-r)\phi \qquad (z = 0). \qquad (6.2a, b)$$

These equations were solved numerically (see Chiareli 1994 for details of the numerical scheme), simultaneously with equation (3.8) for the steady state, to determine the conditions for marginal stability ($\omega = 0$). Checks for consistency were made between the numerical results and the results of the asymptotic theory presented in the last section (Chiareli 1994). Typical eigenfunctions are shown in figure 4, where it can be seen that the upward flow caused by expansion is focused into regions of low permeability, and that this occurs predominantly near the base of the mushy layer. This may be because the basic-state permeability is largest near the base, so the system can gain most advantage by creating channels of low permeability there.

The critical conditions for linear instability are found by tracing the minimum of the neutral curve (cf. figure 2*b*) as it varies with the dimensionless parameters of the system. The results are shown in figure 5.

Firstly, it should be noted that the system is completely stable for $r > 1$, which corresponds to contraction upon solidification. This is because then the flow of interstitial liquid in the mushy layer is in a direction opposite to the temperature gradient. Most pure materials do contract when they solidify, with notable exceptions being water/ice and silicon. However, with an alloy the possibility exists that the solid formed (being depleted of one of the components of the alloy) is less dense than the liquid mixture even though the pure constituents of the alloy would each contract upon

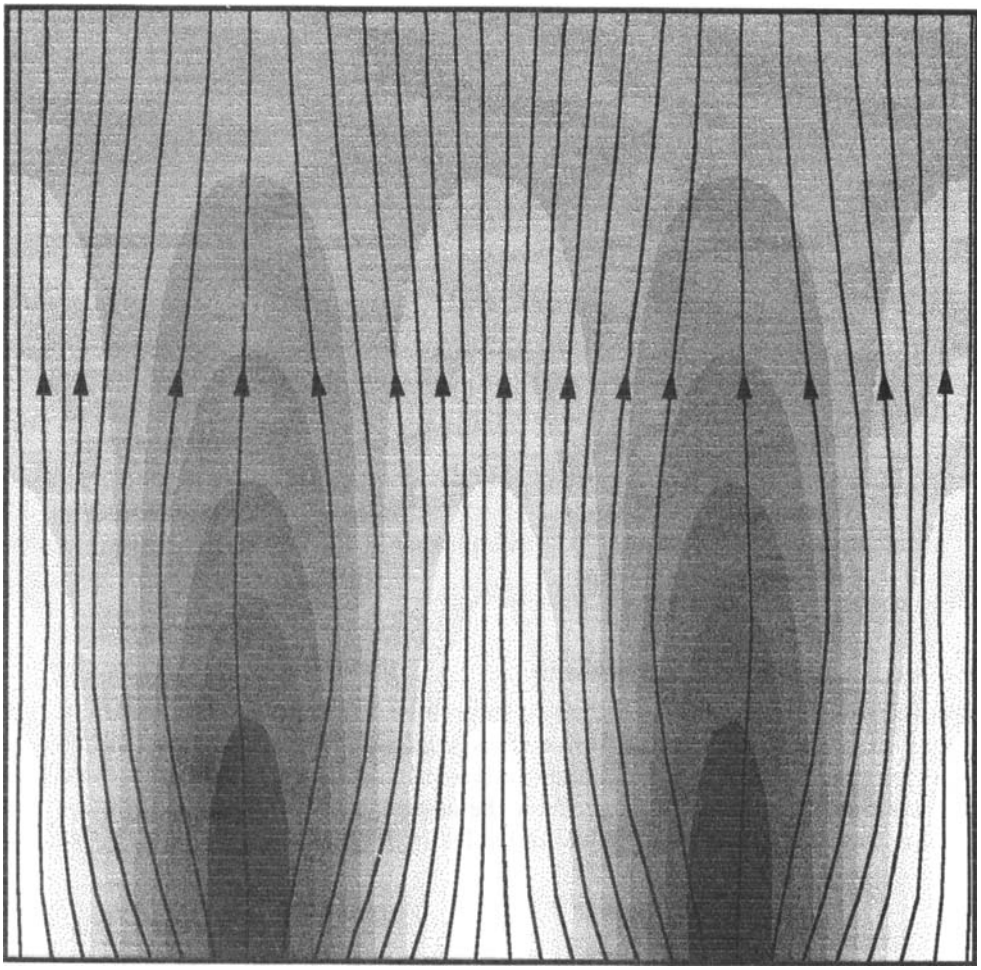

FIGURE 4. Streamlines superimposed on a density plot of the perturbation to the solid fraction in the mushy layer. Light regions correspond to negative perturbations that represent local melting of the dendrites. Darker regions show where solidification is enhanced. The non-dimensional parameter values used in the calculation of these marginal eigenfunctions were $\mathscr{P} = 42$, $\mathscr{S} = \mathscr{C} = \theta_\infty = 1$, and $r = 0.9$.

solidification. For example, the mineral plagioclase is less dense than certain basaltic melts from which it solidifies, even though its constituents individually contract upon solidification. As r decreases below unity, the degree of expansion increases, which strengthens the flow of interstitial liquid parallel to the thermal gradient and renders the system less stable. All this is shown in figure 5(a). It can also be seen that the critical wavenumber becomes large as $r \to 1-$ and the critical value of the sensitivity $\mathscr{P}_c \to \infty$. The numerical results indicate that $\alpha_c \sim \mathscr{P}_c^{1/2}$ in this limit. This can be expressed dimensionally as $\lambda \propto (l_\kappa l_\pi)^{1/2}$, where λ is the wavelength of the critical disturbance, $l_\kappa = \kappa/V$ is the thermal-diffusion lengthscale and l_π is a lengthscale for permeability variations defined by

$$l_\pi = \left[\frac{1}{\Pi}\frac{\mathrm{d}\Pi}{\mathrm{d}\chi}\frac{\mathrm{d}\chi_0}{\mathrm{d}z}\right]^{-1} = \frac{1}{\mathscr{P}}\frac{\chi_0}{\chi_0'}. \tag{6.3}$$

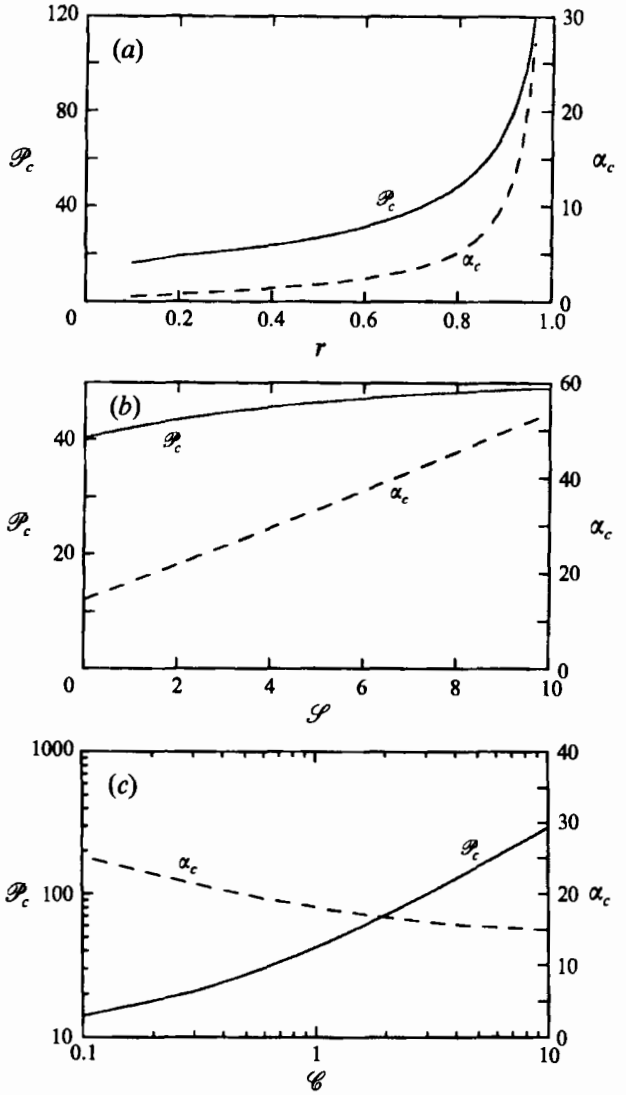

FIGURE 5. The critical conditions $\mathscr{P}_c(\alpha_c)$ for linear stability as functions of the following dimensionless parameters: (*a*) the density ratio r, with $\theta_\infty = \mathscr{C} = \mathscr{S} = 1$; (*b*) the Stefan number $\mathscr{S}$ with $\theta_\infty = \mathscr{C} = 1$ and $r = 0.9$; (*c*) the compositional ratio $\mathscr{C}$, with $\theta_\infty = \mathscr{S} = 1$ and $r = 0.9$.

We see from figure 5(*b*) that the stability of the system is not very sensitive to the value of the Stefan number, though the system becomes slightly more stable as $\mathscr{S}$ increases. This is a combined result of the facts that the depth of the mushy layer decreases as $\mathscr{S}$ increases and that it becomes less reactive.

It was found in the last section that it is necessary that $\mathscr{P} = O(\mathscr{C})$ for instability to occur when $\mathscr{C} \gg 1$. This is seen explicitly in figure 5(*c*), and is because perturbations to the solid fraction, like the solid fraction itself, are small when $\mathscr{C}$ is large.

The overwhelming conclusion of the stability analysis is that, over a wide range of parameter values, the system is only unstable if the sensitivity of the mushy layer $\mathscr{P}$ is rather large. Typical values of $\mathscr{P}$ given for power-law relationships of the form (2.14) are around 2 or 3 depending on the microstructure of the porous medium.

This would suggest that solidifying systems are almost always stable to the focusing mechanisms described by the present analysis. This conclusion might be challenged by the consideration that the permeability can vary much more strongly with porosity when the solid fraction is small. For example, the Kozeny formula gives

$$\Pi \propto \frac{\chi^3}{(1-\chi)^2}, \tag{6.4}$$

which implies that the sensitivity

$$\frac{1}{\Pi}\frac{\mathrm{d}\Pi}{\mathrm{d}\chi} = \frac{3}{\chi} + \frac{2}{1-\chi} \tag{6.5}$$

is large for χ near unity. Note that, although the sensitivity is also large for χ near zero, the flow in that case is small and the system is relatively stable. An additional consideration is that a mushy layer with a highly dendritic microstructure may experience large changes of permeability by the dissolution of a few side branches, which would reduce the solid fraction only a little. The permeability would thus be very sensitive to changes in solid fraction and much more prone to the instability mechanism decribed in this paper.

If such a case were to be studied further, it should be noted that when the liquid fraction is near unity it may no longer be appropriate to use Darcy's law and the mobility ratio $\mathscr{M}$ may no longer be small.

7. Conclusions

We have analysed the stability of the flow of interstitial liquid in a mushy layer driven by expansion or contraction upon solidification. An instability akin to the acid-etching instability in porous rocks was found to occur only in the case of expansion, since only then is the base flow in the same direction as the temperature gradient, which is a necessary condition for flow-induced dissolution within a mushy layer.

The instability is driven by the following positive feedback. If the porosity is locally increased then the permeability there is increased, which allows a greater flow of interstitial fluid. When that flow is in a direction away from the cooled boundary, cool solute-depleted fluid is carried by the flow. There is rapid thermal equilibration within the mushy layer (by thermal diffusion) which allows the fluid then to dissolve the solid crystals around which it flows. The local porosity is thereby increased further and instability may ensue.

Although the potential for instability has been demonstrated mathematically, it was found that the necessary conditions for instability are unlikely to be encountered given typical casting conditions because instability requires that the permeability be a rather strong function of porosity.

We are very grateful for many helpful discussions with John Hinch and John Lister. This work was supported by grants from the National Aeronautics and Space Administration through the Microgravity Science and Applications Division and from the Natural Environment Research Council.

REFERENCES

Amberg, G. & Homsy, G. M. 1993 Nonlinear analysis of buoyant convection in binary solidification with application to channel formation. *J. Fluid Mech.* **252**, 79–98.

Bear, J. 1988 *Dynamics of Fluids in Porous Media.* Dover.

CHADAM, J., HOFF, D., MERINO, E., ORTOLEVA, P. & SEN, A. 1986 Reactive infiltration instabilities. *IMA J. Appl. Maths* **36**, 7–221.

CHEN, F., LU, J. W. & YANG, T. L. 1994 Convective instability in ammonium chloride solution directionally solidified from below. *J. Fluid Mech.* **276**, 163–187.

CHIARELI, A. O. P. 1994 Fluid flow and macrosegregation in mushy layers. PhD thesis, Northwestern University.

CHIARELI, A. O. P, HUPPERT, H. E. & WORSTER, M. G. 1994 Segregation and flow during the solidification of alloys. *J. Cryst. Growth.* **139**, 134–146.

COPLEY, S. M., GIAMEI, A. F., JOHNSON, S. M. & HORNBECKER, M. F. 1970 The origin of freckles in unidirectionally solidified castings *Metall. Trans.* **1**, 2193–2204.

EMMS, P. W. & FOWLER, A. C. 1994 Compositional convection in the solidification of a binary alloy. *J. Fluid Mech.* **262**, 111–139.

FLEMINGS, M. C. 1974 *Solidification Processing.* McGraw Hill.

FOWLER, A. C. 1985 The formation of freckles in binary alloys. *IMA J. Appl. Maths* **35**, 159–174.

HILLS, R. N., LOPER, D. J. & ROBERTS, P. H. 1983 A thermodynamically consistent model of a mushy zone. *Q. J. Appl. Maths* **36**, 505–539.

HINCH, E. J. & BHATT, B. S. 1990 Stability of an acid front moving through porous rock. *J. Fluid Mech.* **212**, 279–288.

SHERWOOD, J. D. 1987 Stability of a plane reaction front in a porous medium. *Chem. Engng Sci.* **42**, No. 7, 1823–1829.

TAIT, S., JAHRLING, K. & JAUPART, C. 1992 The planform of compositional convection and chimney formation in a mushy layer. *Nature* **359**, 406–408.

WORSTER, M. G. 1986 Solidification of an alloy from a cooled boundary. *J. Fluid Mech.* **167**, 481–501.

WORSTER, M. G. 1991 Natural convection in a mushy layer. *J. Fluid Mech.* **224**, 335–359.

WORSTER, M. G. 1992*a* The dynamics of mushy layers. In *Interactive Dynamics of Convection and Solidification* (ed. S. H. Davis, H. E. Huppert, U. Müller & M. G. Worster). NATO ASI **E219**, pp. 113–138. Kluwer.

WORSTER, M. G. 1992*b* Instabilities of the liquid and mushy regions during solidification of alloys. *J. Fluid Mech.* **237**, 649–669.